



This is a repository copy of *Electron spin mediated distortion in metallic systems*.

White Rose Research Online URL for this paper:  
<http://eprints.whiterose.ac.uk/166796/>

Version: Published Version

---

**Article:**

Anand, G., Eisenbach, M., Goodall, R. [orcid.org/0000-0003-0720-9694](https://orcid.org/0000-0003-0720-9694) et al. (1 more author) (2020) Electron spin mediated distortion in metallic systems. *Scripta Materialia*, 185. pp. 159-164. ISSN 1359-6462

<https://doi.org/10.1016/j.scriptamat.2020.04.025>

---

**Reuse**

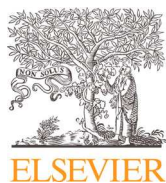
This article is distributed under the terms of the Creative Commons Attribution-NonCommercial-NoDerivs (CC BY-NC-ND) licence. This licence only allows you to download this work and share it with others as long as you credit the authors, but you can't change the article in any way or use it commercially. More information and the full terms of the licence here: <https://creativecommons.org/licenses/>

**Takedown**

If you consider content in White Rose Research Online to be in breach of UK law, please notify us by emailing [eprints@whiterose.ac.uk](mailto:eprints@whiterose.ac.uk) including the URL of the record and the reason for the withdrawal request.



[eprints@whiterose.ac.uk](mailto:eprints@whiterose.ac.uk)  
<https://eprints.whiterose.ac.uk/>



## Electron spin mediated distortion in metallic systems

G. Anand<sup>a,b,c,\*</sup>, Markus Eisenbach<sup>d</sup>, Russell Goodall<sup>b</sup>, Colin L. Freeman<sup>b</sup>

<sup>a</sup> Department of Metallurgy and Materials Engineering, Indian Institute of Engineering Science and Technology-Shibpur, Howrah, WB, India

<sup>b</sup> Department of Materials Science and Engineering, University of Sheffield, UK

<sup>c</sup> Warwick Centre for Predictive Modelling, University of Warwick, UK

<sup>d</sup> Scientific Computing Group, Centre for Computational Sciences, Oak Ridge National Laboratory, Oak Ridge, TN, USA

### ARTICLE INFO

#### Article history:

Received 11 December 2019

Revised 20 April 2020

Accepted 21 April 2020

Available online 18 May 2020

#### Keywords:

High entropy alloys

Distortion

Alloys

Solid solution strengthening

Magnetism

### ABSTRACT

The deviation of positions of atoms from their ideal lattice sites in crystalline solid state systems causes distortion and it causes variation in structural [1] and functional properties [2]. Severe lattice distortion has been proposed to be one of the core-effect in high-entropy alloys. But the fundamental mechanism of distortion at atomic scale is missing for real three-dimensional metallic systems. The present investigation aims to develop mechanistic understanding of atomic scale distortion in metallic systems in terms of the magneto-volume effects. The correlation between charge-disproportion, spin fluctuations, magneto-volume effects and Fermi surface nesting has been highlighted.

© 2020 Acta Materialia Inc. Published by Elsevier Ltd.

This is an open access article under the CC BY-NC-ND license.

(<http://creativecommons.org/licenses/by-nc-nd/4.0/>)

Distortion in metallic systems is a topic of debate in the context of multi-component concentrated alloys or so called “high-entropy alloys (HEAs)” [3–8]. Such distortions are known to influence the structural properties of these alloys [9,10]. Local lattice distortion is instrumental in the determination of elastic properties, where size misfit plays the crucial role by modifying the elastic properties of metallic alloys [11]. Accurate determination of such properties is a key part in developing predictive models for designing newer alloys [12]. HEAs are configurational disordered systems with short-range order in certain cases [13]. CoCrFeMnNi HEA also shows magnetic disorder and spin frustration [14,15]. The chemical and magnetic disorder are the characteristics of such HEAs. Traditionally, influence of chemical and magnetic disorder along with local electronic structure on distortion has been studied with Special Quasi-Random Structure (SQRS) generated supercell. In such scheme supercell is generated to mimic atomic correlation function for perfectly disordered solid solution. Additionally, other schemes such as similar local atomic environment (SLAE) scheme has also been employed to generate random solid solution [1]. SQRS has been particularly employed for studying CoCrFeMnNi [16,17], CoCrFeNi [18,19] and other sub-alloy systems of CoCrFeMnNi. Such studies have pointed towards the significant influence of Cr and Mn on the distortion in CoCrFeMnNi and it should be noted that

influence of such chemical species have been confirmed with combined theoretical and experimental studies [17,20]. In spirit of above, we have carried out structural relaxation of CoCrFeNi HEA and Fig. 1 shows the bond-length distribution which have normal distribution, such distribution for bond-length has also been reported for SQRS generated CoCrFeNi HEA [19]. The inset shows that significant scatter is associated with Cr bonds in comparison with other bonds in CoCrFeNi, which implies that Cr play significant role in distortion in CoCrFeNi HEA. But it should be noted that it is difficult to develop mechanistic picture of interaction of Cr with other alloying elements in the distortion in such metallic alloys.

In view of delineating the elemental influence, we have studied the evolution of distortion with the impurity-in-matrix approach [21] with elements forming the CoCrFeMnNi HEA. We generated an FCC crystal structure for Co, Cr, Fe, Mn and Ni, while a BCC structure was used for Cr, Fe, and Mn. A HCP matrix was generated for Co only. Other elements were added as an impurity in each of the above-stated matrices in the centre of the supercell. Geometry optimisation in Density Functional Theory (DFT) was carried out to determine the equilibrium bond-length between various atoms in the supercell. Fig. 2 shows the histogram of bond-length range for various cases. The bond-length range was determined as the difference between maximum and minimum of the equilibrium bond-length values present in the supercell. We considered this bond-length range as a measure of the distortion in the supercell. In each case it was bond-length values for each atom with its first nearest-neighbour which were determined. It is clear from our results that FCC-Cr with impurities tends to have greater

\* Corresponding author at: Department of Metallurgy and Materials Engineering, Indian Institute of Engineering Science and Technology-Shibpur, Howrah, WB, India.  
E-mail address: [ganand@metal.iests.ac.in](mailto:ganand@metal.iests.ac.in) (G. Anand).

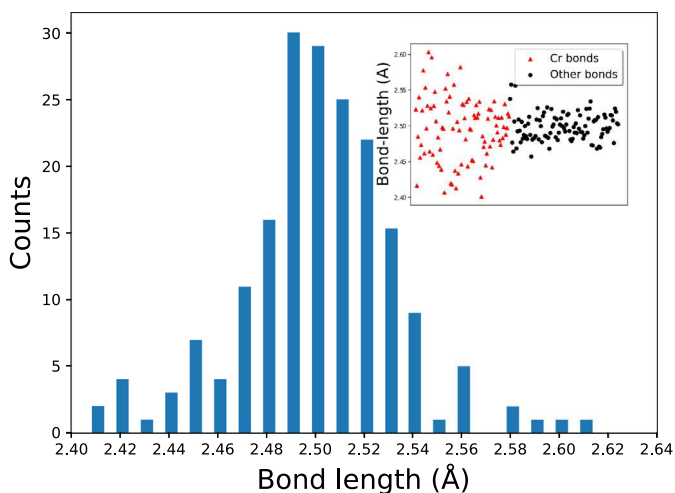


Fig. 1. Bond-length distribution for CoCrFeNi HEA. The inset shows the scatter of bond-length values.

distortion in comparison with the other cases examined. It should be noted that Cr and Mn in multi-component alloys are known to cause maximum distortion [17]. We have plotted spin-isosurfaces for these cases and we found finite spin-polarisation in these systems. It can be seen that Cr at the first nearest-neighbour position tends to have both up and down spin associated with it. It is known that electronic redistribution, spin-flip and change in the bonding structure are correlated in transition metal based systems [22].

We have additionally looked into the charge disproportion and magnetic moment of the impurity atom in the matrix and plotted it with respect to the distortion in the supercell. It can be seen in Fig. 3a that in the case of FCC-Cr, the impurity atom gains electronic charge and the magnetic moment associated with impurities remains close to zero. Such charge-transfer has been reported to be important in atomic-level stress [20,23]. In view of quantifying the influence of the charge disproportion, we have carried out Bader charge analysis, where the net charge on the atom was calculated using Henkelman's grid-based algorithm [24]. After calculation of Bader charge on all atoms in the supercell, we subtracted the Bader charge on a particular atom from the original electronic charge in the pseudopotential to determine the net gain or loss of charge on each atom. It can be seen that impurity atoms in FCC-Cr, tend to gain electronic charge, which is not in the agreement with Pauling's electronegativity scale for Mn in FCC-Cr but rather, Allen's scale provides the correct electronegativity trend for all the cases (see Table 1 in the supplementary information (SI) for electronegativity values). The Allen's scale of electronegativity has been found to be successful for HEAs [25]. Even with net electronic gain on the impurity atoms, interestingly the Bader volume occupied by the impurity atoms seems to be shrinking (Fig. 3b) and such volume misfit has been correlated with distortion [26]. Recent experimental work has also shown that Cr influences the lattice parameter of CoCrFeNi alloy most in comparison with Co, Fe and Ni and hence it exhibits the strongest lattice distortion effect in this alloy [27]. It should be further noted that the impurity-first nearest neighbour bond-length is lower than the bond-length of Cr–Cr pairs.

So to determine the influence of the magnetism on the evolution of distortion, we carried out constrained spin-polarised calculations for the case, where we saw significant distortion (*i.e.*, FCC-Cr with impurities). In these calculations, we forced ferromagnetism on the system by constraining the supercell to have a total initial magnetic moment. We confirmed the imposition of ferromagnetism by determining total electronic density of states (DOS)

(See Fig. 2 in the SI), which shows the exchange split in up and down spin for constrained ferromagnetic calculations. It can be clearly seen that forcing ferromagnetism causes the reduction of distortion (Fig. 3c) as well as reduction in volume-shrinkage associated with the impurity atoms in the supercell (Fig. 3d). Such observation points towards a correlation between volume shrinkage and distortion in such systems. The correlation of volume shrinkage and reduction in the bond-length between substitutional solute and Cr explains the local distortion (or negative strain) observed when 3d transition metals are alloyed with another transition metal [21]. Also, it can be seen that forcing ferromagnetism in FCC-Cr system leads to the lower charge disproportion on the impurity atom and higher magnetic moment. Additionally, we found two magnetic ground-states for FCC-MnCr (*i.e.*, Cr in FCC-Mn); first with a high magnetic moment associated with Cr and Mn (high spin state) with higher distortion 0.12 Å and a second one with lower magnetic moment with lower distortion (0.036 Å). The characteristic of distortion in the case of FCC-MnCr (*i.e.*, Cr impurity in FCC-Mn) is different from as that seen in the case of FCC-Cr matrix. In the case of the FCC-Cr matrix, distortion takes place at impurity-Cr bonds, while in the case of FCC-MnCr, Mn–Mn interaction causes the distortion. The Bader analysis similarly showed the discrepancy in the volume associated with Mn, which is minimised in the case of low magnetic moment case (Fig. 3e).

As stated above, substitutional alloying in FCC-Cr leads to finite spin polarisation in the system or the magnetic moment associated with the FCC-Cr matrix atoms and impurity atom has some finite value. The range of magnetic moment associated with FCC-Cr with impurity supercell is  $-0.004$  to  $0.001 \mu_B$  for FCC-CrCo (Co impurity in FCC-Cr),  $-0.018$  to  $0.038 \mu_B$  for FCC-CrFe (Fe impurity in FCC-Cr),  $-0.168$  to  $0.016 \mu_B$  for FCC-CrMn (Mn impurity in FCC-Cr) and  $-0.0002$  to  $0.0004 \mu_B$  for FCC-CrNi (Ni impurity in FCC-Cr). We visualised the Kohn-Sham orbitals in the plane of the impurity. We found the fluctuation in the magnetic moment of Kohn-Sham states between the impurity and Cr in the FCC-Cr matrix. Such fluctuation is absent in the case of ferromagnetic systems (see Fig. 3(a) (a) and 4 in SI). Additionally such fluctuation was also seen in the case of high spin FCC-MnCr, where significant distortion is seen (Fig. 3(b) and (c) in SI). To ensure that such fluctuation might not be due to numerical noise, we studied the fluctuation at various k-points (Fig. 6 in SI). It is clear that the ratio of the magnetic moment of conduction Kohn-Sham states and that of impurity atom remains close to  $10^{-3}$ . We additionally contracted and expanded the supercell of the FCC-CrCo system and carried out electronic minimisation to the effect of lattice movement on the appearance of the fluctuation in the magnetic moment of the conduction Kohn-Sham states. We observed that when the system was contracted by 0.93 of the equilibrium volume (Fig. 7(a) in SI), the spin fluctuations were still present suggesting a link to the relaxation of the atoms towards each other in the general case. Expansion of the system removed the presence of the fluctuation again suggesting that this effect is linked to the localised distortion of atoms moving closer together within the cell. Therefore the fluctuation appears to be a screening behaviour between the conduction Kohn-Sham states. It should also be noted that such fluctuations are closely correlated with the atomic movement. In view of influence of conduction Kohn-Sham states in the above-stated cases, we generated the Fermi surfaces for FCC-CrCo, FCC-CrFe, FCC-CrMn and FCC-CrNi. These calculations were carried out using a larger supercell with 108 atoms. We observed the parallel sheets of the Fermi surfaces (Fig. 4) in each case. In Fig. 4 we also show a two-dimensional cross section of the Fermi surfaces for all cases which have been obtained from sectioning the three-dimensional surface parallel to the (020) plane. The parallel sheets to Fermi surface are quantified in terms of vector for which the sheets are parallel. This phenom-

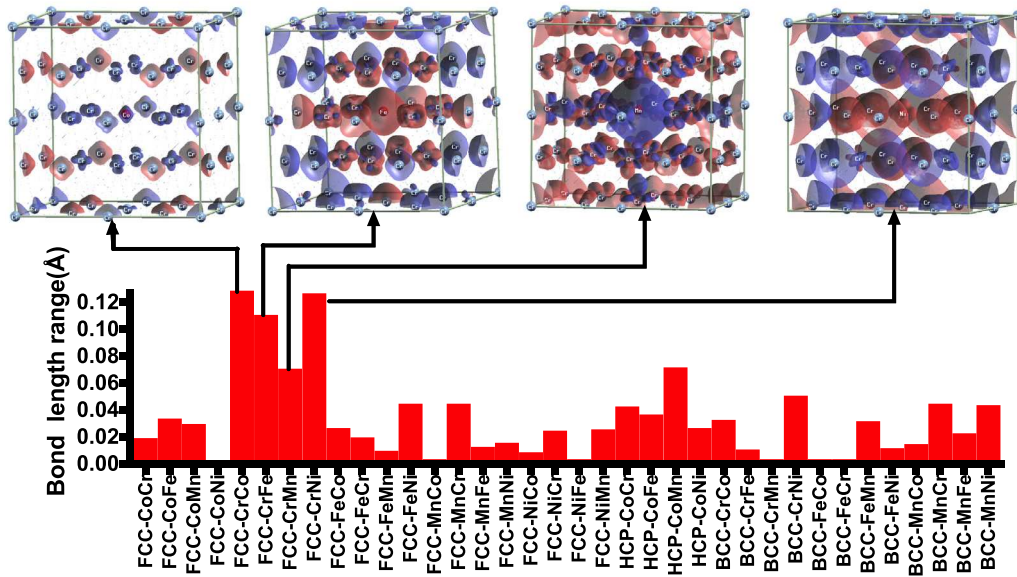


Fig. 2. Variation in the bond distortion for various cases, spin iso-surface for Cr matrix has been added showing Cr with both up and down spin.

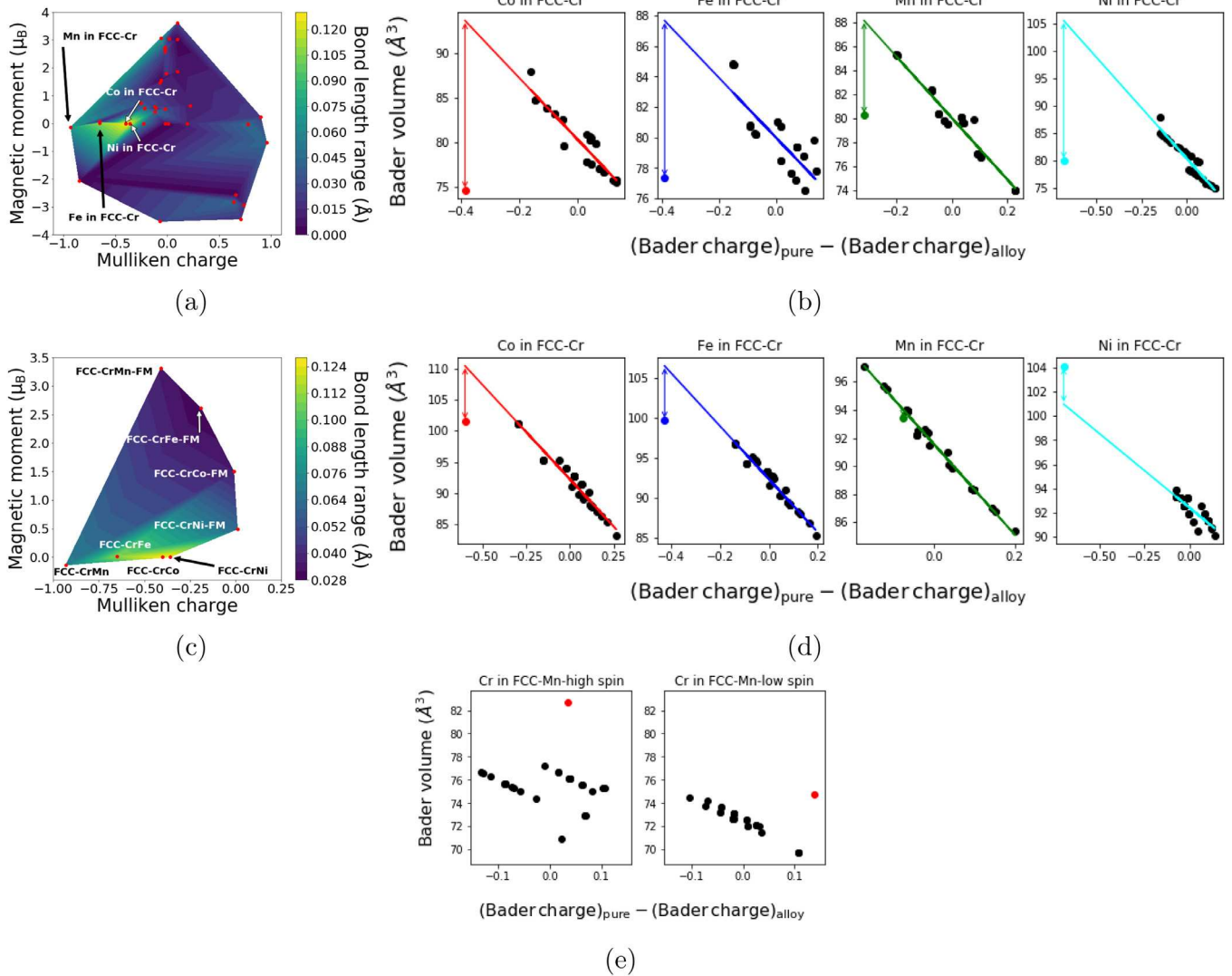
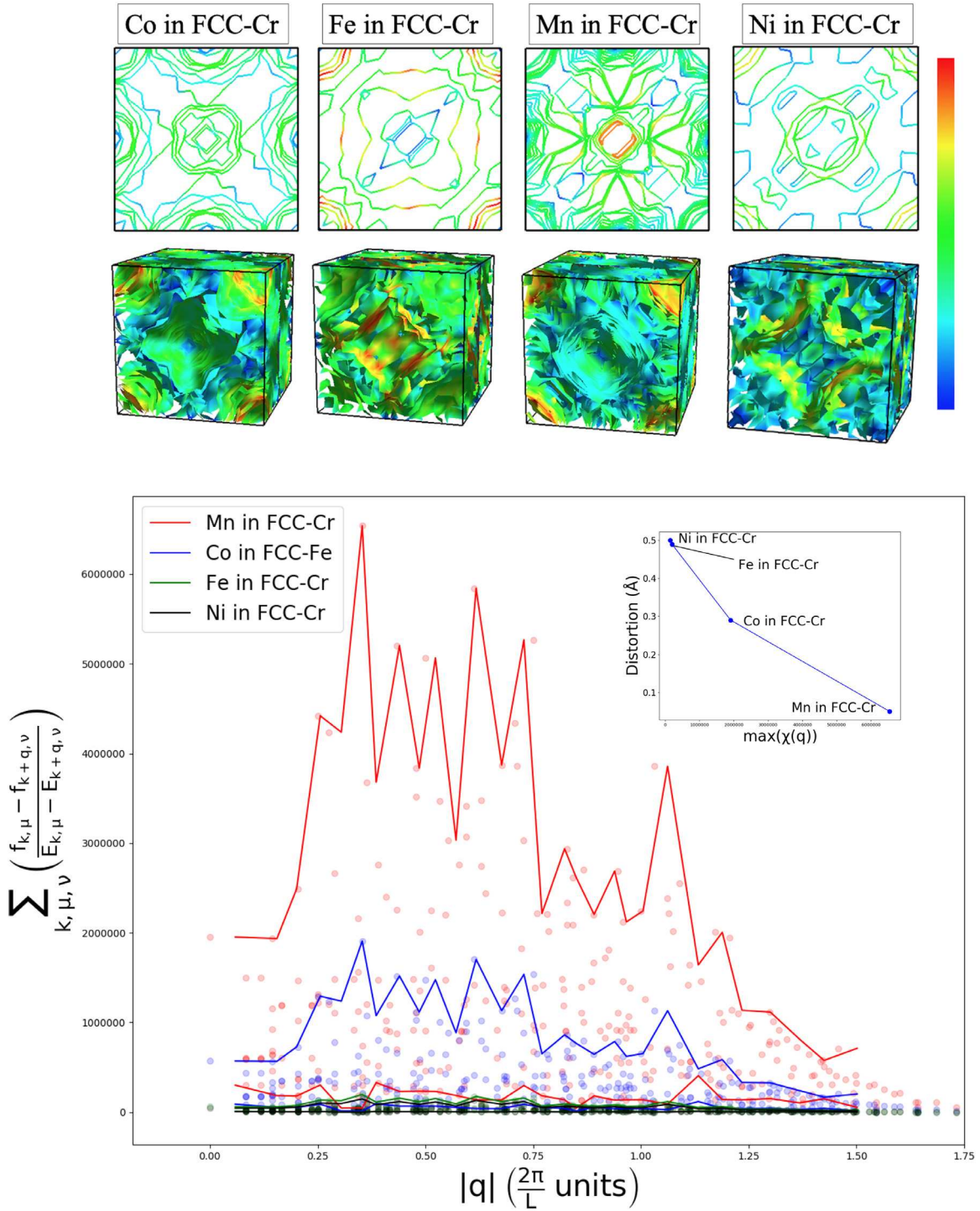


Fig. 3. (a) Variation of Mulliken charge, magnetic moment of impurity and distortion in the supercell. The qualitative agreement between Mulliken and Bader charge is presented in Fig. 1 of SI. (b) Bader volume associated with net Bader charge of impurity and matrix (c) Change in Mulliken charge, magnetic moment of the impurity and consequent change in distortion for ferromagnetic system (d) Bader volume associated with net Bader charge for impurity and matrix elements for ferromagnetic case (e) Bader volume associated with Mn and impurity Cr atoms with respect to net charge for high spin (high magnetic moment) and low spin (low magnetic moment) case.



**Fig. 4.** Fermi Surface topology for Co, Fe, Mn and Ni in FCC-Cr (drawn using FermiSurfer), along with response function for each of these cases. The inset in the figure show the maximum value of response function with distortion in the supercell.

ena is known as Fermi surface nesting and the above-stated vector is the nesting vector ( $q$ ). To quantify the Fermi surface nesting, we determined the response function ( $\chi(q)$ ) [28] as,

$$\chi(q) = \sum_{k, \mu, \nu} \left( \frac{f_{k, \mu} - f_{k+q, \nu}}{E_{k, \mu} - E_{k+q, \nu}} \right) \quad (1)$$

where,  $\mu$  and  $\nu$  are band indices, while  $f$  is occupancy factor, which is zero above the Fermi energy and one below the Fermi energy. The results across the cell are shown Fig. 4. The inset of Fig. 4 shows the linear correlation of  $\max(\chi(q))$  with distortion,

where systems with lower Fermi surface nesting have higher distortion. In pure Cr in the BCC state, Overhauser predicted spin density wave (SDW) [29], while Lomer suggested that the SDW is enhanced if Fermi surface nesting is present [30]. Also, Marcus et al., showed that strain waves (sinusoidal variation of strain) due to the magneto-volume effect may also stabilise SDW [31]. So, it can be stated that Fermi surface nesting and distortion in pure Cr are positively correlated. In our investigation for FCC-Cr with impurity, we have found a negative correlation between Fermi surface nesting and distortion. In our case, Co, Fe and Ni in FCC-Cr

lead to the ferromagnetic ordering with fluctuating spin at the interstices, while antiferromagnetic ordering is present in the case of Mn in FCC-Cr. It is clear that spin fluctuations are mediating the magneto-volume effects (*i.e.*, volume shrinkage). It can be understood that above-stated mechanisms involving charge-transfer and magnetic characteristics lead to the magneto-volume effects. Additionally a correlation between distortion due to the magneto-volume effect and Fermi surface topology has been presented for the simple cases. But, it should be noted that such effects such as fluctuation in atomic volumes and charge transfer have been reported for the concentrated multicomponent HEA [32]. Recent experimental work [33] has shown that Fermi surface features survive even in the presence of disorder in the case of CoCrFeNi HEA. Such report points towards the applicability the mechanistic picture presented above in the case of impurity-in-matrix calculations for complex concentrated alloys.

In summary, the present investigation shows the correlation between charge disproportion, spin-flip, Fermi surface nesting with the distortion in metallic systems. We have observed the volume shrinkage of the valence electron cloud, which leads to the reduction of equilibrium bond-length between metallic elements. Such volume shrinkage is related to the magnetic ground-state along with the screening effects of conduction electrons. It has also been shown that distortion and Fermi surface nesting are negatively correlated. This study provides a fundamental description of distortion in three dimensional metallic systems which will be relevant for the design of newer alloys with attractive structural properties.

## Method

DFT calculations were performed using the CASTEP code [34], which uses a plane-wave expansion of one-electron wave functions. Ultrasoft pseudopotential were used to define the electron-ion interaction [35]. The electron exchange-correlation was defined using the generalised gradient approximation [36] with a Perdew-Burke-Ernzerhof functional [37]. Spin-polarised calculations were carried out to introduce magnetism. Geometric optimisation was carried out in all the cases to obtain the statically relaxed structure with tolerance values for ionic displacement, force on ions, stress on ions set to 0.001 Å, 0.05 Å, and 0.1 GPa, respectively. The geometric relaxation was carried out without imposing any constraints to determine the magnetic ground state of the system. The DFT calculations were performed with the supercell approach with the impurity-in-matrix methodology which means that a different element is added to the centre of the supercell of a pure elemental system. The FCC structure was modelled for Co, Cr, Fe, Mn and Ni, while a BCC structure for Cr, Fe and Mn was generated. The HCP structure for Co was generated as well. A 2x2x2 supercell was generated for BCC, FCC and HCP cases, containing 16, 32 and 16 atoms respectively. In each of these cases, the remaining elements are added as a perturbation substitutionally to determine their individual effect on the bond-lengths to characterise the influence of individual elements on distortion in alloys. The plane wave cut-off ( $E_{\text{cut}}$ ) for Co, Cr, Fe, Mn and Ni were determined to be 500 eV, 700 eV, 500 eV, 700 eV and 500 eV, respectively. The number of k-points for Brillouin-zone integration was determined from convergence testing to be  $10^3$ ,  $12^3$ ,  $10^3$  and  $12^3$  for Co, Cr, Fe, Mn and Ni, respectively. In the case of matrix-in-impurity calculations, higher  $E_{\text{cut}}$  and k-points were chosen. Additionally, 3x3x3 supercell containing 108 atoms was employed for FCC-Cr matrix with Co, Fe, Mn and Ni impurity was carried out as well with  $E_{\text{cut}}$  of 700 eV, 600 eV, 600 eV, and 700 eV, respectively. A 10x10x10 k-points grid was used for 3x3x3 supercell calculations. A 2x2x2 supercell for the CoCrFeNi HEA was constructed by random placement of the atoms on the lattice sites. Calculations were performed with a  $E_{\text{cut}}$  of 600 eV and 10x10x10 k-points.

## Data and code availability

Raw data associated with the publication may be provided by authors on request.

## Declaration of Competing Interest

The authors declare that they have no known competing financial interests or personal relationships that could have appeared to influence the work reported in this paper.

## Acknowledgments

GA is thankful to Phil Hasnip and Keith Refson for helpful discussions, University of Sheffield for PhD scholarship and Leverhulme trust for funding postdoctoral research under Grant RPG-2017-191. GA and CLF are thankful for support provided via our membership of the UK's HPC Materials Chemistry Consortium, which is funded by EPSRC (EP/L000202) and GA is also thankful to computing facilities through UKCP consortium with EPSRC grant reference EP/P022065/1. Additional computing facilities were provided by the Scientific Computing Research Technology Platform of the University of Warwick. The work of ME has been supported by U.S. Department of Energy, Office of Science, Basic Energy Sciences, Material Sciences and Engineering Division and it used resources of the Oak Ridge Leadership Computing Facility, which is a DOE Office of Science User Facility supported under Contract DE-AC05-00OR22725.

## Supplementary material

Supplementary material associated with this article can be found, in the online version, at doi:10.1016/j.scriptamat.2020.04.025.

## References

- [1] H. Song, F. Tian, Q.-M. Hu, L. Vitos, Y. Wang, J. Shen, N. Chen, *Phys. Rev. Mater.* (2017), doi:10.1103/PhysRevMaterials.1.023404.
- [2] D. Berardan, A.K. Meena, S. Franger, C. Herrero, N. Dragoe, *J. Alloy. Compd.* (2017), doi:10.1016/j.jallcom.2017.02.070.
- [3] E.P. George, D. Raabe, R.O. Ritchie, *Nature Reviews Materials* 4 (7–8) (2019), doi:10.1038/s41578-019-0121-4. 515–
- [4] C. Lee, G. Song, M.C. Gao, R. Feng, P. Chen, J. Brechtel, Y. Chen, K. An, W. Guo, J.D. Poplawsky, S. Li, A.T. Samaei, W. Chen, A. Hu, H. Choo, P.K. Liaw, *Acta Mater.* 160 (2018) 158–172, doi:10.1016/j.actamat.2018.08.053.
- [5] W.M. Choi, Y.H. Jo, S.S. Sohn, S. Lee, B.J. Lee, *npj Comput. Mater.* 4 (2018), doi:10.1038/s41524-017-0060-9.
- [6] Y. Tong, K. Jin, H. Bei, J.Y. Ko, D.C. Pagan, Y. Zhang, F.X. Zhang, *Mater. Des.* 155 (2018) 1–7, doi:10.1016/j.matdes.2018.05.056.
- [7] W. Song, A. Radulescu, L. Liu, W. Bleck, *Steel Res. Int.* 87 (2017), doi:10.1002/srin.201700079.
- [8] L.R. Owen, N.G. Jones, *J. Mater. Res.* 33 (19) (2018) 2954–2969, doi:10.1557/jmr.2018.322.
- [9] Q. He, Y. Yang, *Front. Mater.* 5 (2018).
- [10] B. Feng, M. Widom, *Mater. Chem. Phys.* 210 (2018) 309–314, doi:10.1016/j.matchemphys.2017.06.038.
- [11] G. Kim, H. Diao, C. Lee, A. Samaei, T. Phan, M. de Jong, K. An, D. Ma, P.K. Liaw, W. Chen, *Acta Mater.* (2019).
- [12] G.P.M. Leyson, W.A. Curtin, L.G. Hector Jr, C.F. Woodward, *Nat. Mater.* 9 (9) (2010) 750.
- [13] C. Niu, A. Zaddach, A. Oni, X. Sang, J. Hurt III, J. LeBeau, C. Koch, D. Irving, *Appl. Phys. Lett.* 106 (16) (2015) 161906.
- [14] O.c.v. Schneeweiss, M. Friák, M. Dudová, D. Holec, M. Šob, D. Krieger, V. Holý, P.c.v. Beran, E.P. George, J. Neugebauer, A. Dlouhý, *Phys. Rev. B* 96 (2017) 014437, doi:10.1103/PhysRevB.96.014437.
- [15] Z. Dong, S. Schönecker, W. Li, D. Chen, L. Vitos, *Sci. Rep.* 8 (1) (2018) 1–7.
- [16] Y. Ye, Y. Zhang, Q. He, Y. Zhuang, S. Wang, S. Shi, A. Hu, J. Fan, Y. Yang, *Acta Mater.* 150 (2018) 182–194.
- [17] H.S. Oh, D. Ma, G.P. Leyson, B. Grabowski, E.S. Park, F. Kormann, D. Raabe, *Entropy* 18 (2016) 321, doi:10.3390/e18090321.
- [18] Y. Tong, S. Zhao, K. Jin, H. Bei, J. Ko, Y. Zhang, F. Zhang, *Scr. Mater.* 156 (2018) 14–18.
- [19] Y. Tong, G. Velisa, S. Zhao, W. Guo, T. Yang, K. Jin, C. Lu, H. Bei, J. Ko, D. Pagan, Y. Zhang, L. Wang, F. Zhang, *Materialia* 2 (2018) 73–81.

- [20] H.S. Oh, S.J. Kim, K. Odbadrakh, W.H. Ryu, K.N. Yoon, S. Mu, F. Körmann, Y. Ikeda, C.C. Tasan, D. Raabe, T. Egami, E.S. Park, *Nat. Commun.* 10 (2019) 2090, doi:[10.1038/s41467-019-10012-7](https://doi.org/10.1038/s41467-019-10012-7).
- [21] M. Morinaga, *A Quantum Approach to Alloy Design: an Exploration of Material Design and Development Based Upon Alloy Design Theory and Atomization Energy Method*, Elsevier, 2019, doi:[10.1016/b978-0-12-814706-1.00011-x](https://doi.org/10.1016/b978-0-12-814706-1.00011-x).
- [22] W.Y. Wang, S.L. Shang, Y. Wang, Y.J. Hu, K.A. Darling, L.J. Kecskes, S.N. Mathaudhu, X.D. Hui, Z.K. Liu, *Mater. Chem. Phys.* 162 (2015) 748–756, doi:[10.1016/j.matchemphys.2015.06.051](https://doi.org/10.1016/j.matchemphys.2015.06.051).
- [23] Y. Tong, S. Zhao, H. Bei, T. Egami, Y. Zhang, F. Zhang, *Acta Mater.* 183 (2020) 172–181.
- [24] W. Tang, E. Sanville, G. Henkelman, *J. Phys.* 21 (8) (2009) 84204, doi:[10.1088/0953-8984/21/8/084204](https://doi.org/10.1088/0953-8984/21/8/084204).
- [25] M.G. Poletti, L. Battezzati, *Acta Mater.* 75 (2014) 297–306.
- [26] W.G. Nöhning, W.A. Curtin, *Scr. Mater.* 168 (2019) 119–123, doi:[10.1016/j.scriptamat.2019.04.012](https://doi.org/10.1016/j.scriptamat.2019.04.012).
- [27] Z. Wang, Q. Wu, W. Zhou, F. He, C. Yu, D. Lin, J. Wang, C.T. Liu, *Scr. Mater.* 162 (2019) 468–471, doi:[10.1016/j.scriptamat.2018.12.022](https://doi.org/10.1016/j.scriptamat.2018.12.022).
- [28] R. Gupta, S. Sinha, *Phys. Rev. B* 3 (8) (1971) 2401.
- [29] A. Overhauser, *Phys. Rev.* 128 (3) (1962) 1437.
- [30] W. Lomer, *Proc. Phys. Soc.* 80 (2) (1962) 489.
- [31] P. Marcus, S. Qiu, V. Moruzzi, *J. Phys.* 10 (29) (1998) 6541.
- [32] S. Ishibashi, Y. Ikeda, F. Körmann, B. Grabowski, J. Neugebauer, *Phys. Rev. Mater.* 4 (2020) 23608, doi:[10.1103/PhysRevMaterials.4.023608](https://doi.org/10.1103/PhysRevMaterials.4.023608).
- [33] H.C. Robarts, T.E. Millichamp, D.A. Lagos, J. Laverock, D. Billington, J.A. Duffy, D. O'Neill, S.R. Giblin, J.W. Taylor, G. Kontrym-Sznajd, M. Samsel-Czekala, H. Bei, S. Mu, G.D. Samolyuk, G.M. Stocks, S.B. Dugdale, *Phys. Rev. Lett.* 124 (2020) 046402, doi:[10.1103/PhysRevLett.124.046402](https://doi.org/10.1103/PhysRevLett.124.046402).
- [34] S.J. Clark, M.D. Segall, C.J. Pickard, P.J. Hasnip, M.I. Probert, K. Refson, M.C. Payne, *Z. Kristallogr.* 220 (5/6) (2005) 567–570, doi:[10.1524/zkri.220.5.567.65075](https://doi.org/10.1524/zkri.220.5.567.65075).
- [35] D. Vanderbilt, *Phys. Rev. B* 41 (1990) 7892–7895, doi:[10.1103/PhysRevB.41.7892](https://doi.org/10.1103/PhysRevB.41.7892).
- [36] D.R. Hamann, M. Schlüter, C. Chiang, *Phys. Rev. Lett.* 43 (1979) 1494–1497, doi:[10.1103/PhysRevLett.43.1494](https://doi.org/10.1103/PhysRevLett.43.1494).
- [37] J.P. Perdew, K. Burke, M. Ernzerhof, *Phys. Rev. Lett.* 77 (1996) 3865–3868, doi:[10.1103/PhysRevLett.77.3865](https://doi.org/10.1103/PhysRevLett.77.3865).